Electronic Supplementary Material (ESI) for CrystEngComm.

Supporting Information

Two donor-acceptor (D-A) type Zn(II) complexes as fluorescent probes for highly selective detection of iodide

Hao Su, Liang Hao, Wajid Hussain, Zhongkui Li and Hui Li*[a]

[a] *Key Laboratory of Cluster Science of Ministry of Education, School of Chemistry and Chemical Engineering, Beijing Institute of Technology, Beijing 100081, P. R. China*

*E-mail: lihui@bit.edu.cn

Table of Content

nm) spectra of complex **2** (1.0×10^{-5} mol L^{-1}) in various solvents.

Fig. S13. PL emission spectra of complex (a) **1** and (b) **2** with various ions (Br^-, Cl^-, F^-, SO_4^{2-}, SO_3^{2-}, $S_2O_3^{2-}$, CO_3^{2-}, HCO_3^-, $P_2O_7^{2-}$, $C_2O_4^{2-}$) of 100 equivalents compared with iodide ions of 20 equivalents in THF and H_2O (99:1) (**1**: λ_{ex} = 595 nm; **2**: λ_{ex} = 575 nm).

Fig. S14. PL emission spectra of $\mathbf{L^1}$ with iodide ions of 20 equivalents in THF and H_2O (99:1) (λ_{ex} = 365 nm).

Fig. S15. PL emission spectra of complex (a) **1** and (b) **2** with iodide ions and addition of silver nitrate in THF and H_2O (99:1) (**1**: λ_{ex} = 595 nm; **2**: λ_{ex} = 575 nm).

Fig. S16. ESI-MS spectra of complex (a) **1** and (b) **2** with excess iodide and addition of silver nitrate in MeCN solution.

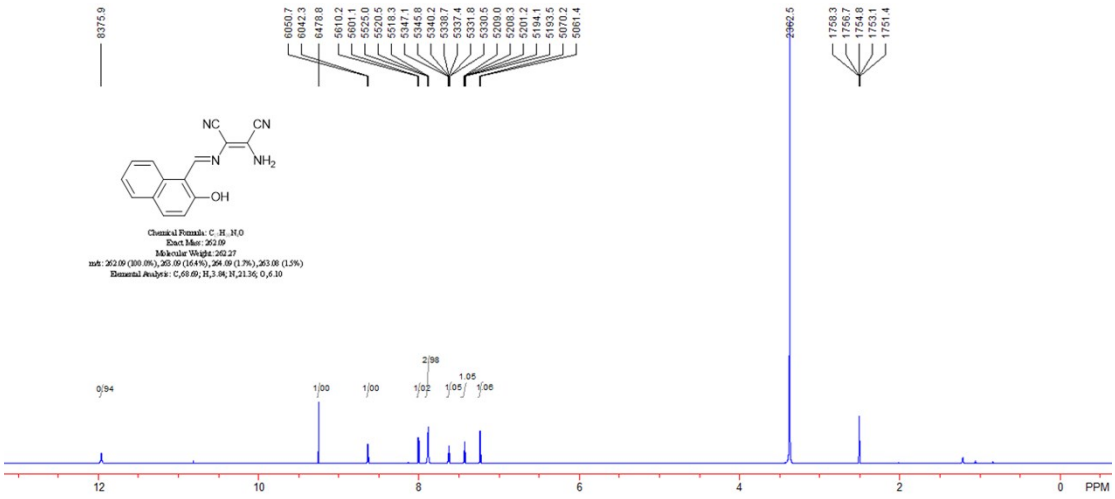

Fig. S1. ^{1}H NMR of (a) **L^{1}**.

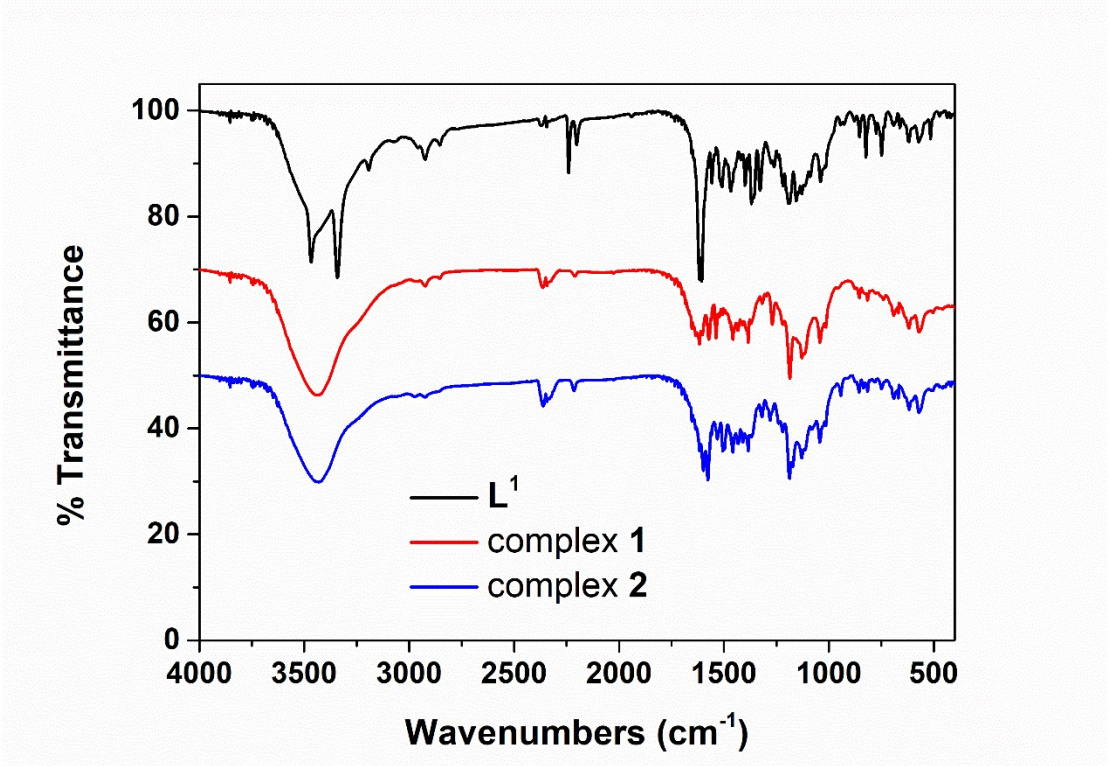

Fig. S2. IR spectra of **L^{1}**, complex **1** and complex **2**.

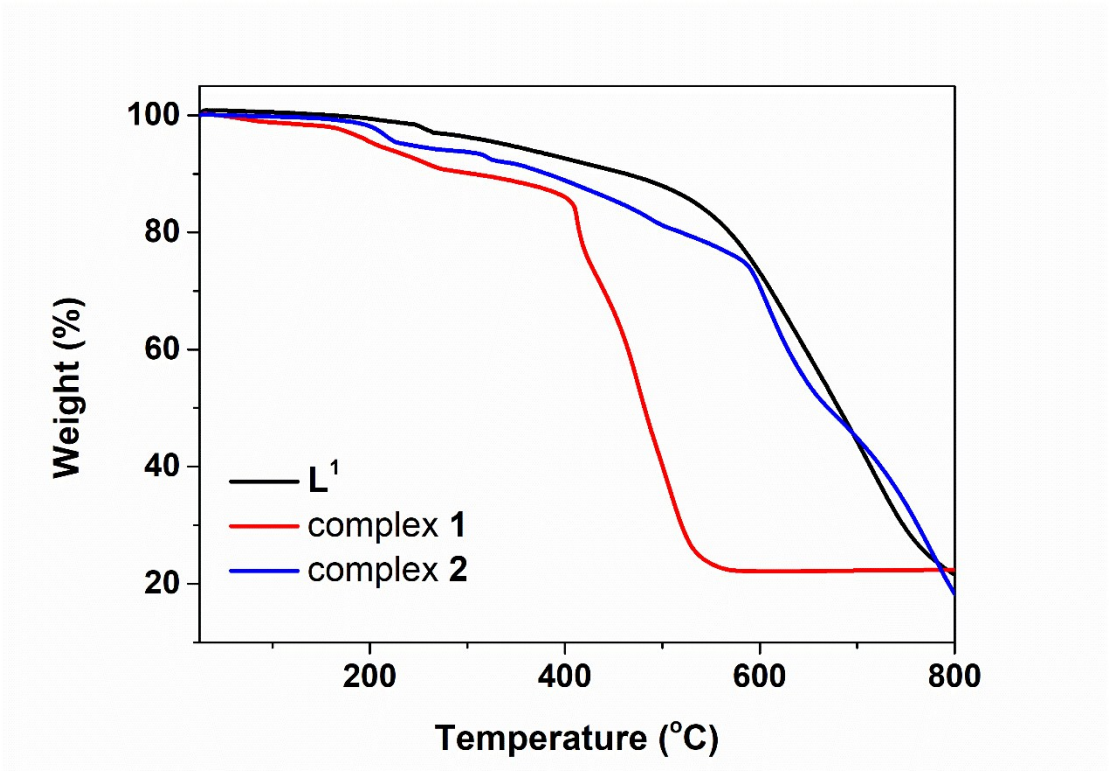

Fig. S3. TG curves of $\mathbf{L^1}$, complex **1** and complex **2**.

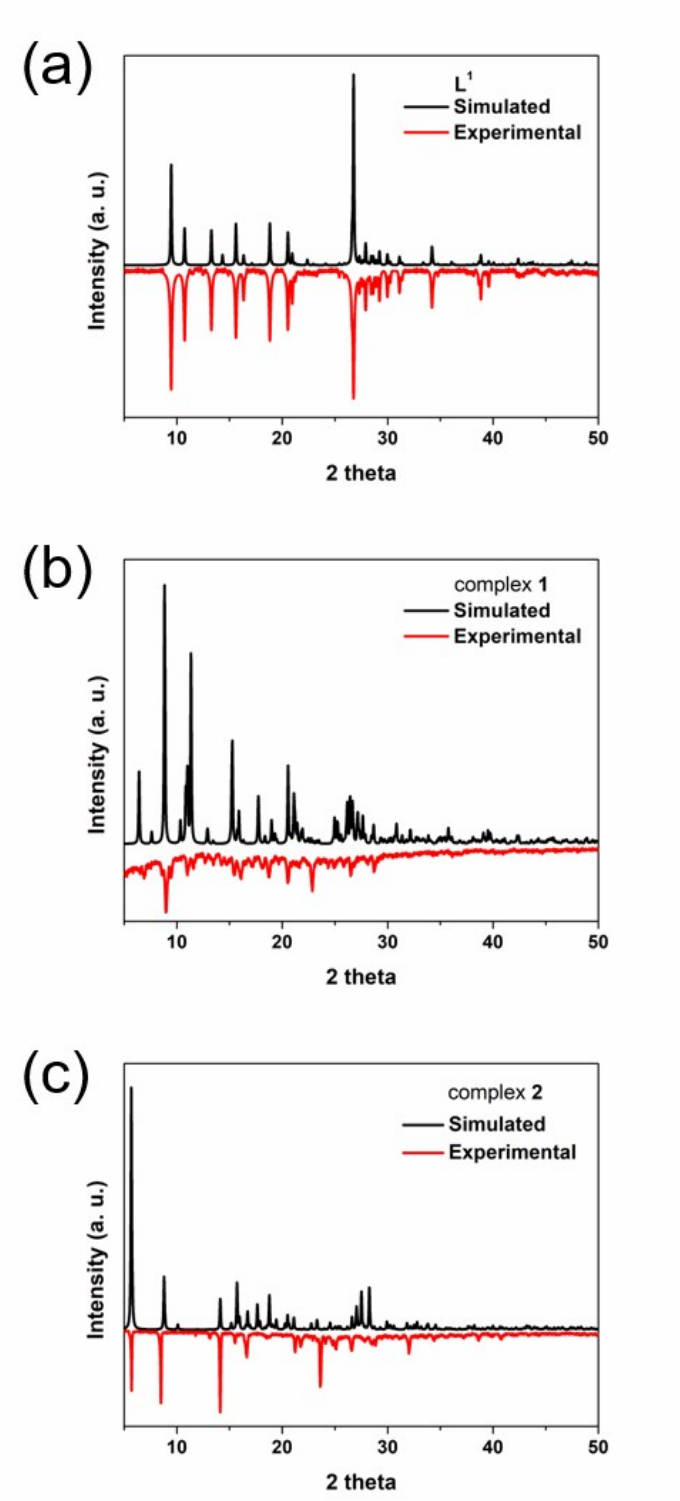

Fig. S4. PXRD patterns show the comparison between the experimental value and calculated ones for (a) **L**[1]; (b) complex **1**; (c) complex **2**.

Table S1. Crystallographic Data for **L[1]**, **1** and **2**.

Complex	**L[1]**	**1**	**2**
Formula	$C_{15}H_{10}N_4O$	$C_{35}H_{26}N_{10}O_3Zn_2$	$C_{22}H_{13}ClN_4O_3Zn$
Mr	262.27	765.40	482.18
Crystal system	Orthorhombic	Triclinic	Monnoclinic
Space group	$P2_12_12_1$	*P*-1	$P2_1/n$
a (Å)	6.6568(17)	10.2417(4)	6.0468(7)
b (Å)	11.350(3)	12.1827(5)	31.046(3)
c (Å)	16.471(3)	14.1173(6)	10.7876(12)
α (°)	90	77.388(10)	90
β (°)	90	88.119(10)	100.317(4)
γ (°)	90	77.243(10)	90
V(Å^3)	1244.5(5)	1676.29(12)	1992.4(4)
Z	4	2	4
F(000)	544	780	976
Reflections used	1348	6430	2127
Independent reflections	2992	8294	3431
Goodness-of-fit on F^2	1.091	1.047	1.059
R_{int}	0.0824	0.0204	0.1018
$R_1[I>2\sigma(I)]$	0.0750	0.0284	0.0544
$wR_2[I>2\sigma(I)]$	0.1514	0.0719	0.1026
R_1(all data)	0.1699	0.0433	0.1096
wR_2(all data)	0.1780	0.0773	0.1217

Table S2. Selected bond distances (Å) and angles (°) for **L[1]**.

O(1)–C(7)	1.346(5)	N(1)–C(1)	1.154(7)
N(2)–C(3)	1.139(6)	N(3)–C(2)	1.336(6)
N(4)–C(4)	1.392(5)	N(4)–C(5)	1.304(5)
C(1)–C(2)	1.423(7)	C(2)–C(4)	1.356(6)
C(3)–C(4)	1.422(6)	C(5)–C(6)	1.428(6)
C(6)–C(7)	1.376(6)	C(6)–C(11)	1.446(6)
C(7)–C(8)	1.405(6)	C(8)–C(9)	1.350(7)
C(9)–C(10)	1.398(7)	C(10)–C(11)	1.418(6)
C(10)–C(15)	1.401(7)	C(11)–C(12)	1.399(6)
C(12)–C(13)	1.359(7)	C(13)–C(14)	1.389(7)
C(14)–C(15)	1.356(8)		
C(4)–N(4)–C(5)	120.0(4)	N(1)–C(1)–C(2)	175.8(6)
N(3)–C(2)–C(1)	114.8(4)	N(3)–C(2)–C(4)	125.2(4)
C(1)–C(2)–C(4)	120.0(4)	N(2)–C(3)–C(4)	177.5(6)
N(4)–C(4)–C(2)	118.9(4)	N(4)–C(4)–C(3)	121.5(4)
C(2)–C(4)–C(3)	119.6(4)	N(4)–C(5)–C(6)	122.2(4)
C(5)–C(6)–C(7)	121.2(4)	C(5)–C(6)–C(11)	119.9(4)

C(7)–C(6)–C(11)	118.9(4)	O(1)–C(7)–C(6)	122.7(4)
O(1)–C(7)–C(8)	115.2(4)	C(6)–C(7)–C(8)	122.0(4)
C(7)–C(8)–C(9)	119.0(5)	C(8)–C(9)–C(10)	122.4(5)
C(9)–C(10)–C(11)	119.4(4)	C(9)–C(10)–C(15)	120.6(5)
C(11)–C(10)–C(15)	119.9(5)	C(6)–C(11)–C(10)	118.2(4)
C(6)–C(11)–C(12)	124.3(4)	C(10)–C(11)–C(12)	117.5(4)
C(11)–C(12)–C(13)	121.0(5)	C(12)–C(13)–C(14)	121.3(5)
C(13)–C(14)–C(15)	119.5(5)	C(10)–C(15)–C(14)	120.7(5)

Table S3. Selected bond distances (Å) and angles (°) for complex **1**.

Zn(1)–O(1)	2.0475(12)	Zn(1)–O(2)	2.0413(11)
Zn(1)–N(6)	2.0058(15)	Zn(1)–O(7)	2.1124(15)
Zn(1)–N(10)	2.0885(17)	Zn(2)–O(1)	2.0090(12)
Zn(2)–O(2)	2.0464(11)	Zn(2)–O(3)	2.0582(14)
Zn(2)–N(1)	2.1012(14)	Zn(2)–N(2)	2.0016(16)
O(1)–Zn(1)–O(2)	76.92(5)	O(1)–Zn(1)–N(6)	151.72(6)
O(2)–Zn(1)–N(6)	104.98(5)	O(2)–Zn(1)–N(7)	146.40(5)
O(2)–Zn(1)–N(10)	102.23(6)	N(6)–Zn(1)–N(7)	81.11(6)
N(6)–Zn(1)–N(10)	107.51(6)	N(7)–Zn(1)–N(10)	107.35(6)
O(1)–Zn(2)–O(2)	77.67(5)	O(1)–Zn(2)–O(3)	100.39(6)
O(1)–Zn(2)–N(1)	152.51(5)	O(1)–Zn(2)–N(2)	108.08(6)
O(2)–Zn(2)–O(3)	98.86(6)	O(2)–Zn(2)–N(1)	84.28(5)
O(2)–Zn(2)–N(2)	156.51(6)	O(3)–Zn(2)–N(1)	102.76(6)
O(3)–Zn(2)–N(2)	102.30(7)	N(1)–Zn(2)–N(2)	81.23(6)

Table S4. Selected bond distances (Å) and angles (°) for complex **2**.

Zn(1)–O(1)	1.974(3)	Zn(1)–O(2)	1.977(3)
Zn(1)–O(3)	2.082(3)	Zn(1)–N(1)	2.083(4)
Zn(1)–N(4)	2.050(4)		
O(1)–Zn(1)–O(2)	96.93(14)	O(1)–Zn(1)–O(3)	99.47(14)
O(1)–Zn(1)–N(1)	89.15(15)	O(1)–Zn(1)–N(4)	157.03(15)
O(2)–Zn(1)–O(3)	96.61(14)	O(2)–Zn(1)–N(1)	160.96(15)
O(2)–Zn(1)–N(4)	87.83(15)	O(3)–Zn(1)–N(1)	100.18(14)
O(3)–Zn(1)–N(4)	102.29(14)	N(1)–Zn(1)–N(4)	79.90(16)

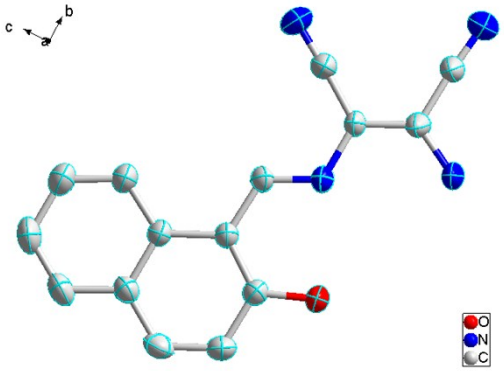

Fig. S5. ORTEP picture of $\mathbf{L^1}$.

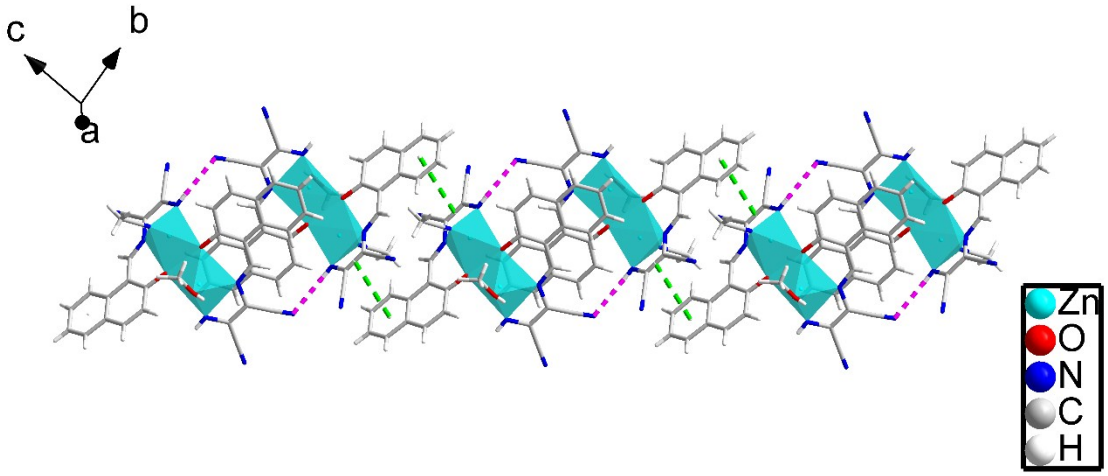

Fig. S6. 1D chain crystal structure of complex **1** via π-π interaction.

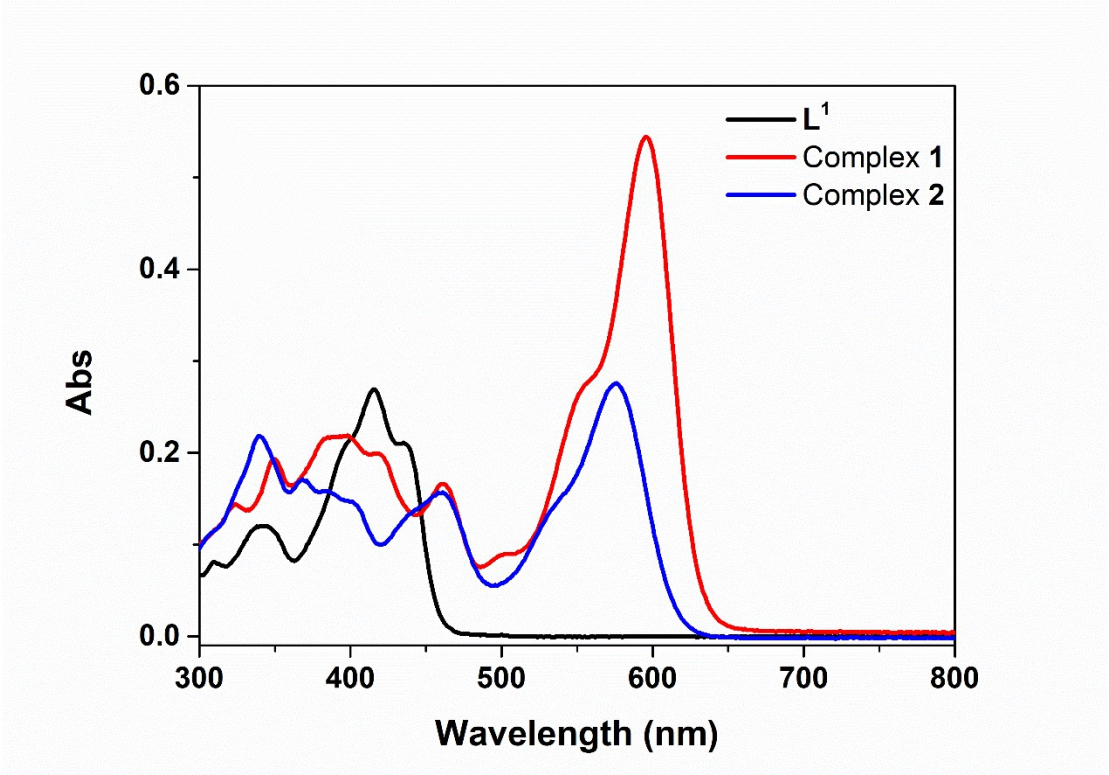

Fig. S7. The UV-visible spectra of **L**[1], complex **1** and complex **2** in THF solution (1.0 × 10^{-5} mol L^{-1}).

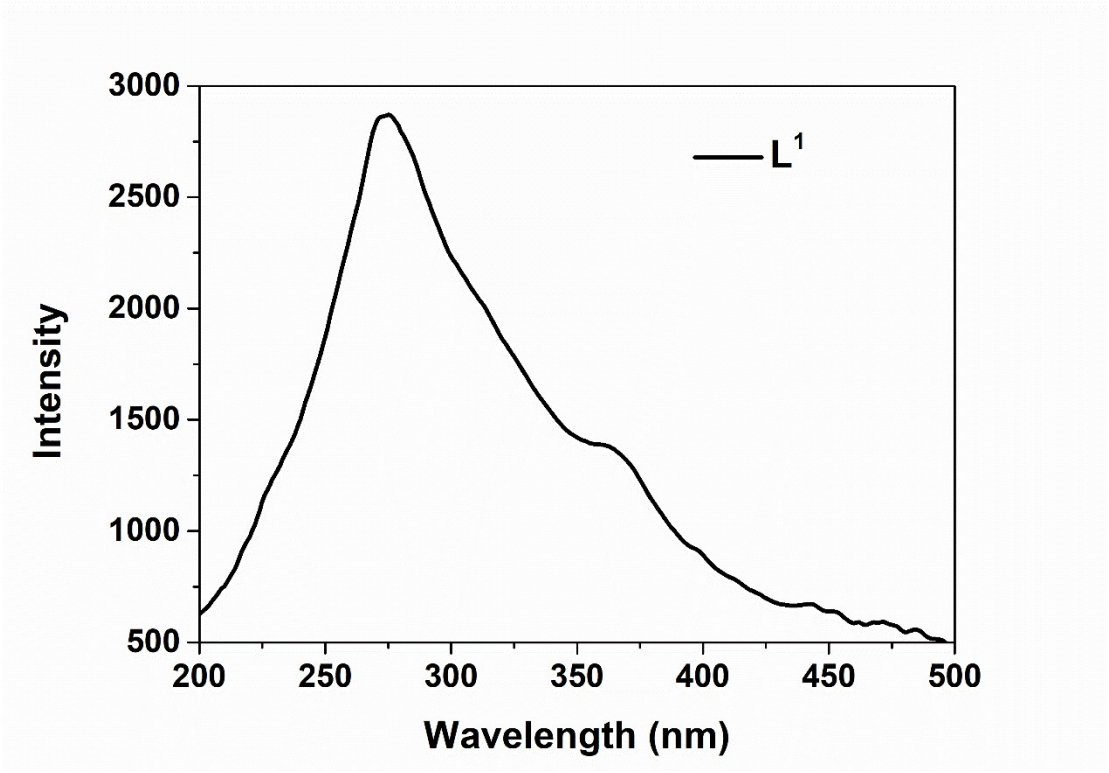

Fig. S8. Excitation spectra of $\mathbf{L^1}$ at solid state.

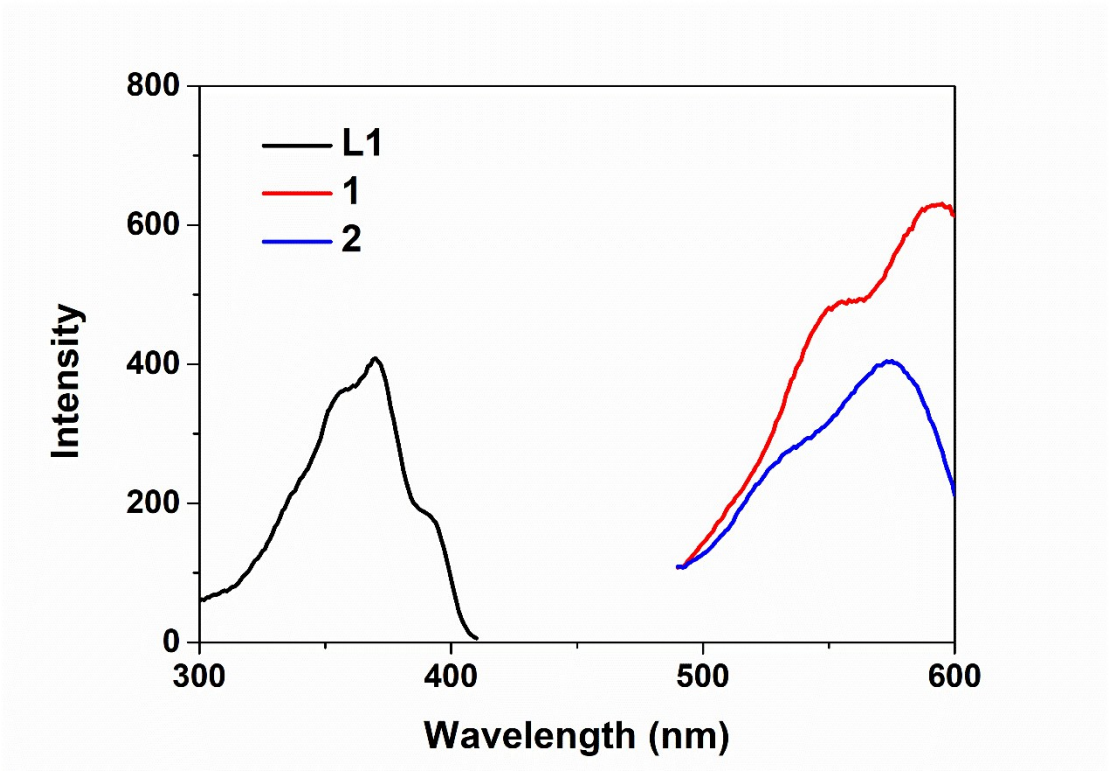

Fig. S9. Excitation spectra of $\mathbf{L^1}$ complex **1** and **2** in THF solution (1.0×10^{-5} mol L^{-1}).

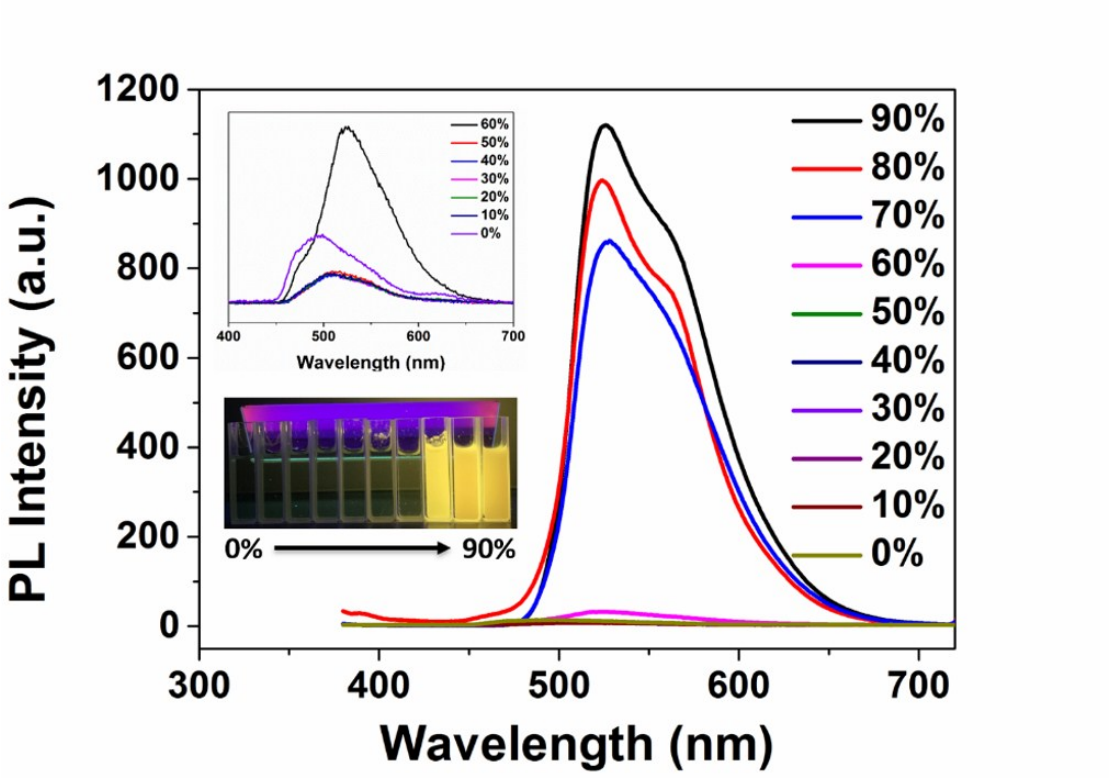

Fig. S10. Emission spectra of **L**[1] in THF and H_2O mixture solution with different water fractions with a concentration of 1.0×10^{-4} M (λ_{ex} = 365 nm); The picture was unified taken at 365 nm under an ultraviolet light.

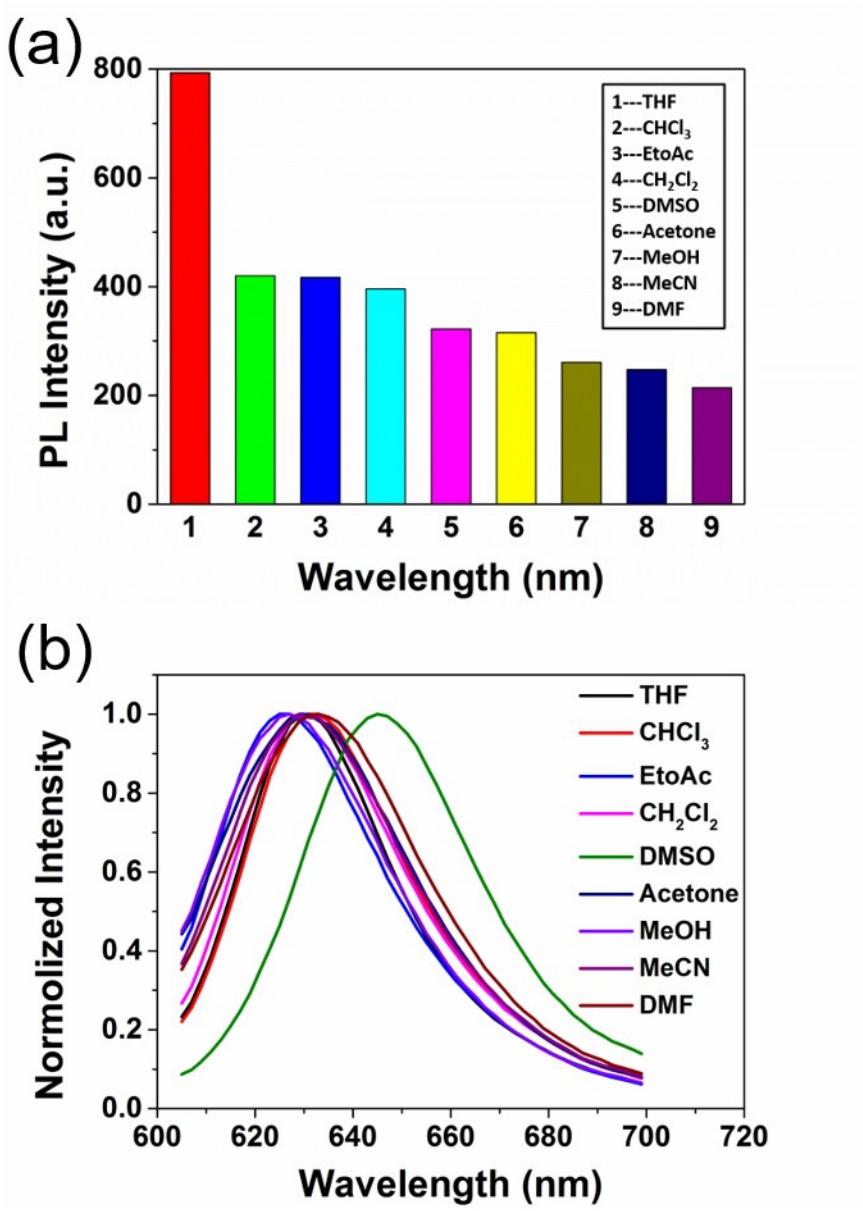

Fig. S11. (a) The change in the fluorescence (λ_{ex} = 365 nm) intensity of complex **1** (1.0 × 10^{-5} mol L^{-1}) in various solvents. (b) The normalized fluorescent (λ_{ex} = 365 nm) spectra of complex **1** (1.0 × 10^{-5} mol L^{-1}) in various solvents.

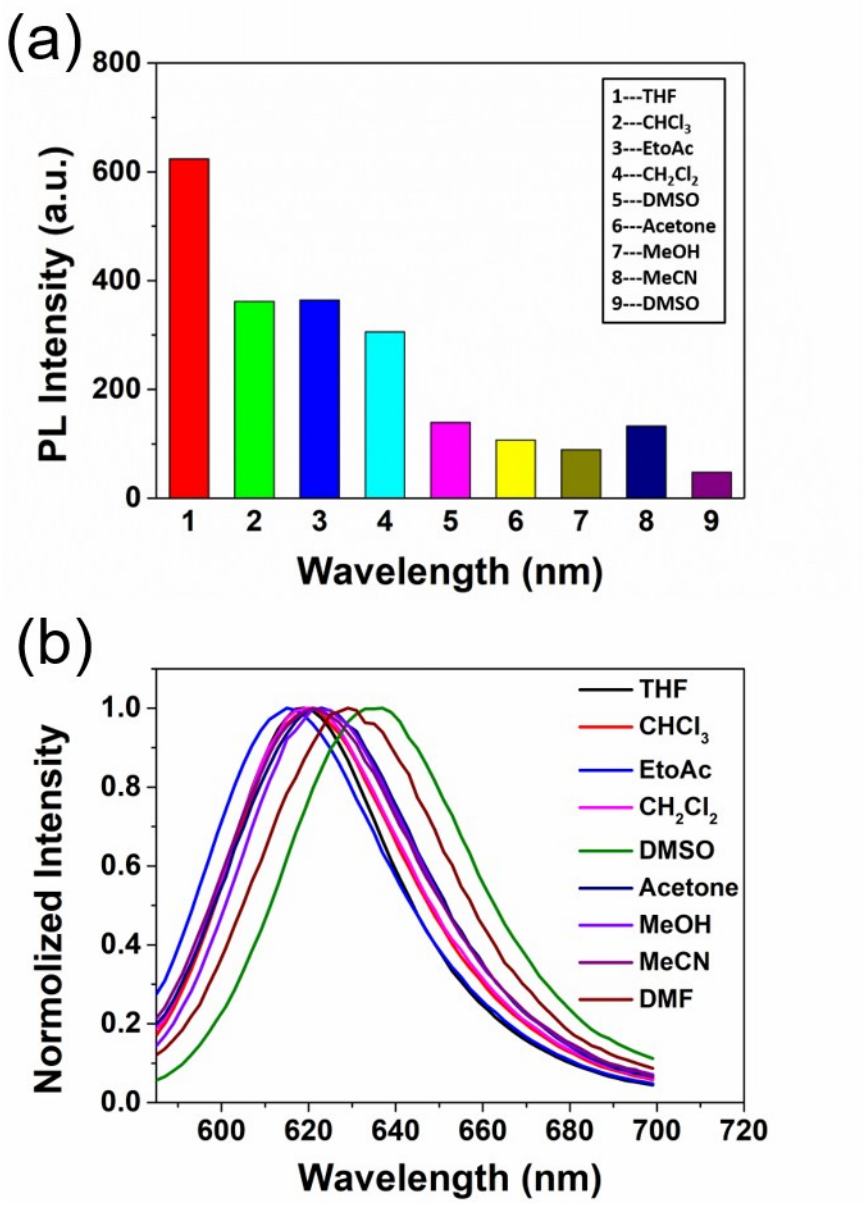

Fig. S12. (a) The change in the fluorescence (λ_{ex} = 365 nm) intensity of complex **2** (1.0 × 10^{-5} mol L^{-1}) in various solvents. (b) The normalized fluorescent (λ_{ex} = 365 nm) spectra of complex **2** (1.0 × 10^{-5} mol L^{-1}) in various solvents.

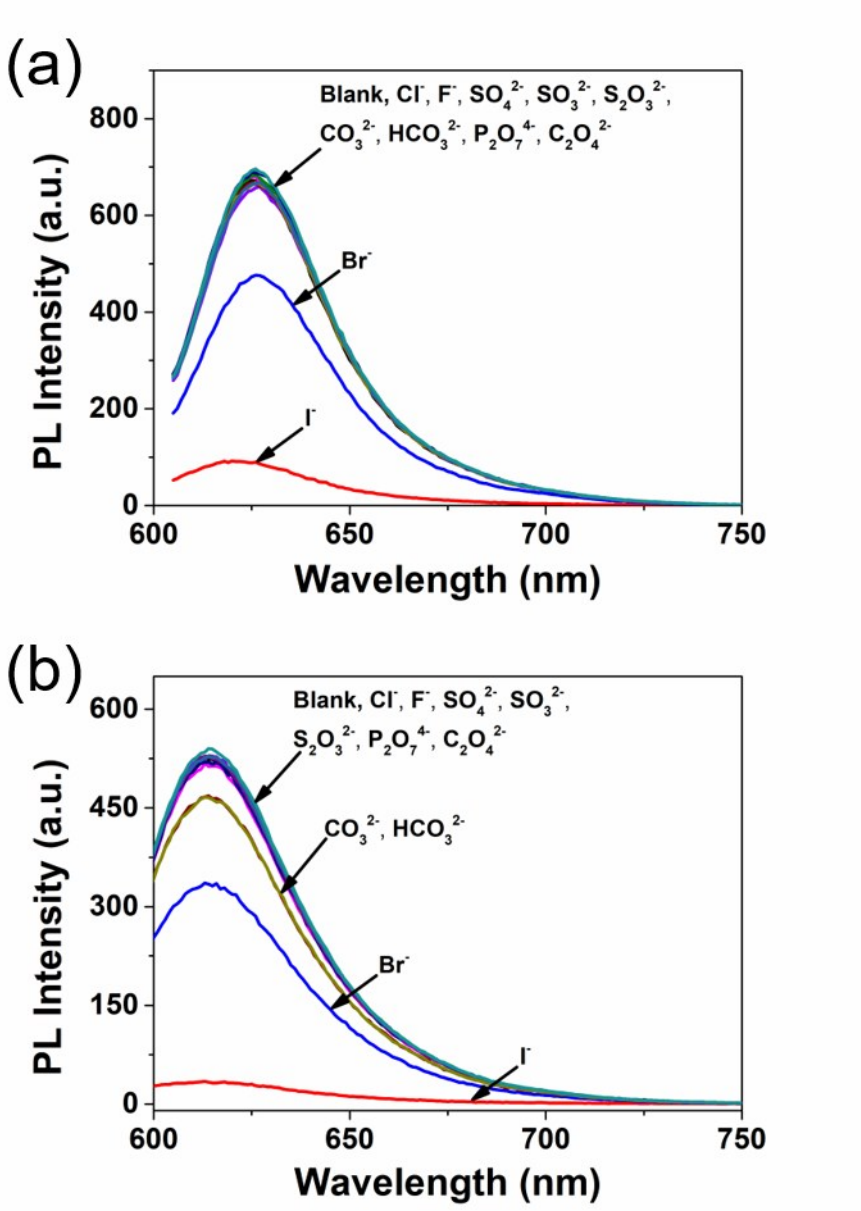

Fig. S13. PL emission spectra of complex (a) **1** and (b) **2** with various ions (Br^-, Cl^-, F^-, SO_4^{2-}, SO_3^{2-}, $S_2O_3^{2-}$, CO_3^{2-}, HCO_3^-, $P_2O_7^{2-}$, $C_2O_4^{2-}$) of 100 equivalents compared with iodide ions of 20 equivalents in THF and H_2O (99:1) (**1**: λ_{ex} = 595 nm; **2**: λ_{ex} = 575 nm).

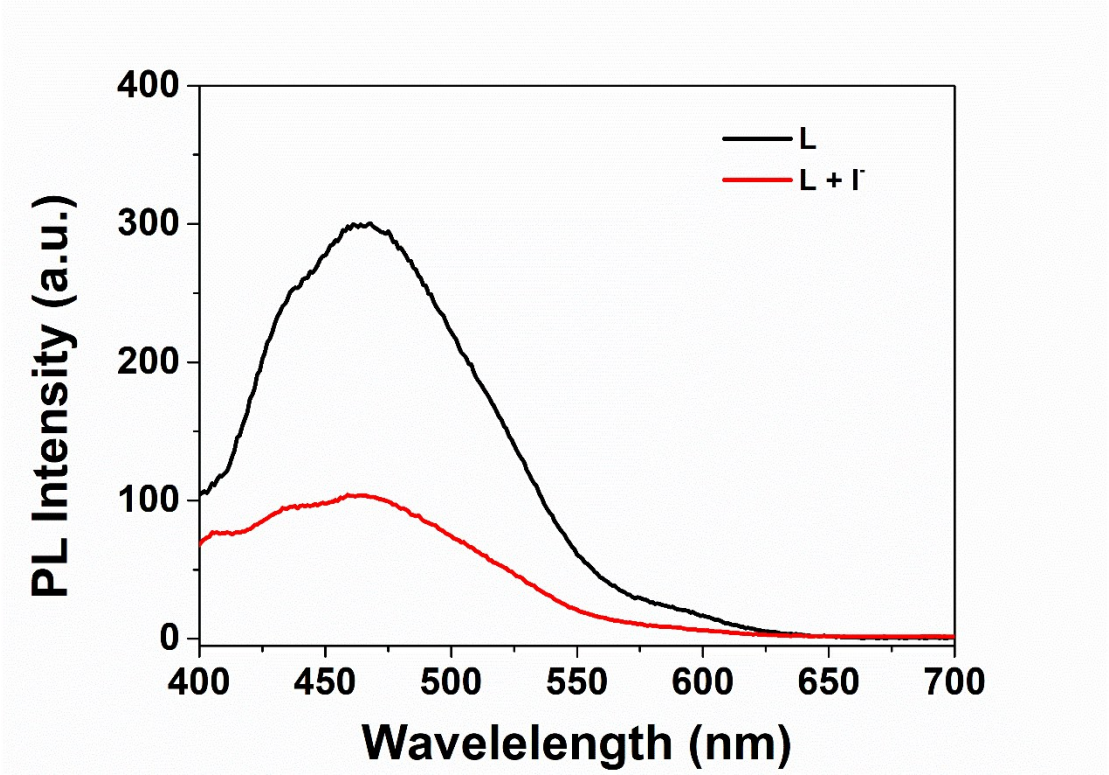

Fig. S14. PL emission spectra of $\mathbf{L^1}$ with iodide ions of 20 equivalents in THF and H_2O (99:1) (λ_{ex} = 365 nm).

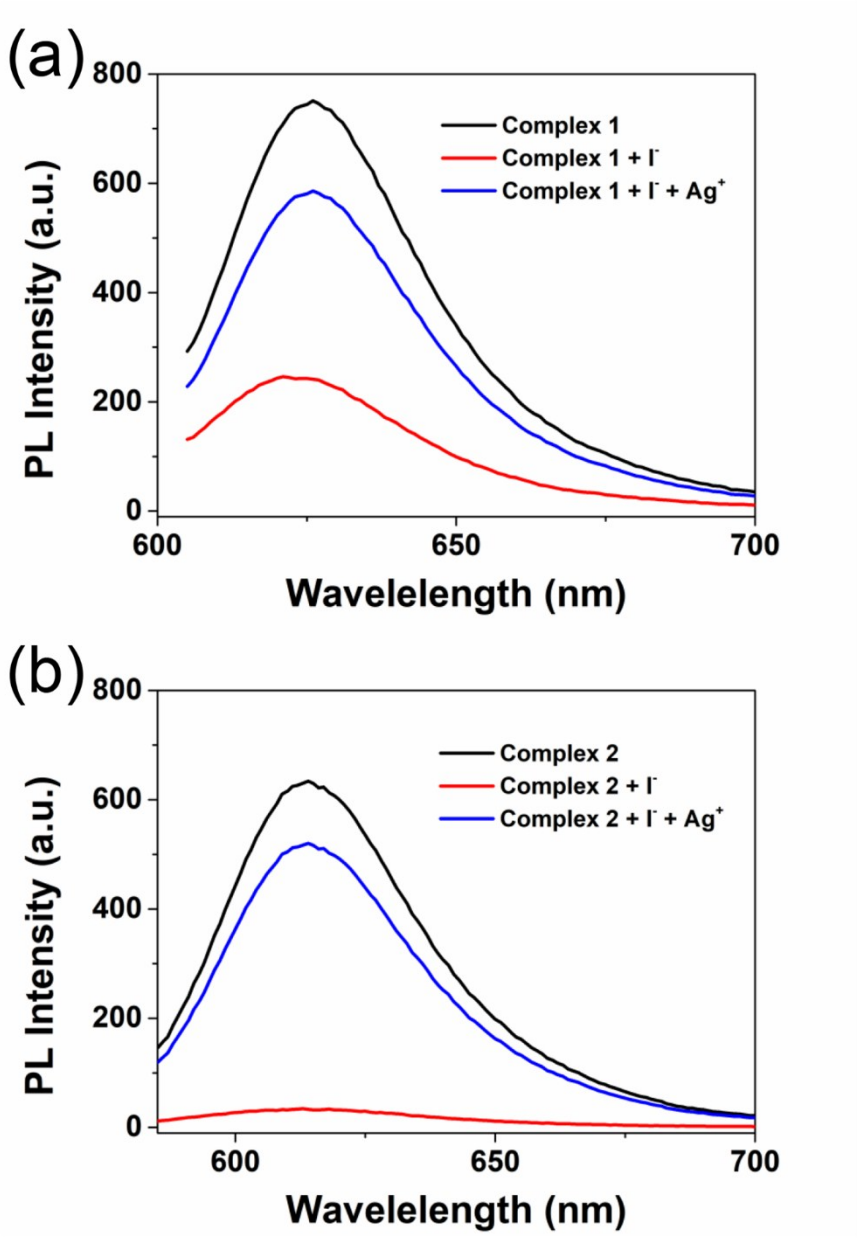

Fig. S15. PL emission spectra of complex (a) **1** and (b) **2** with iodide ions and addition of silver nitrate in THF and H_2O (99:1) (**1**: λ_{ex} = 595 nm; **2**: λ_{ex} = 575 nm).

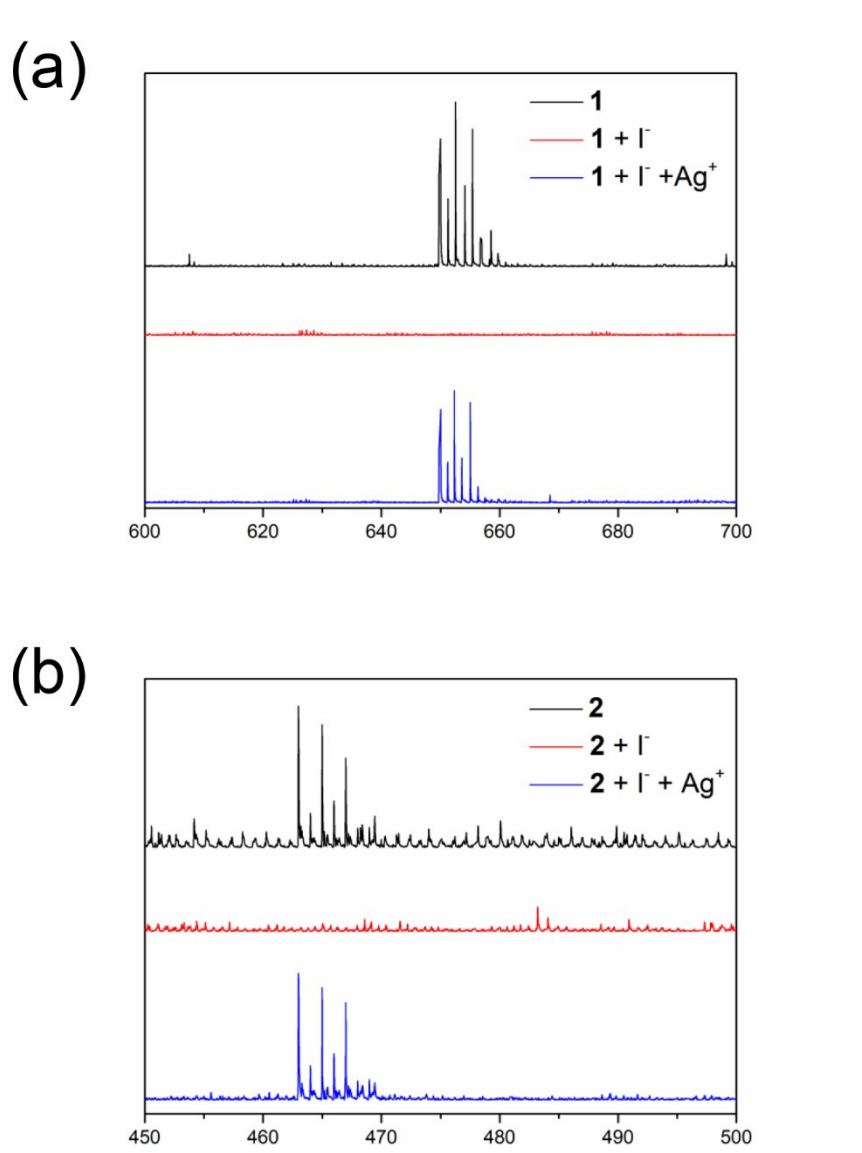

Fig. S16. ESI-MS spectra of complex (a) **1** and (b) **2** with excess iodide and addition of silver nitrate in MeCN solution.